Vibration Analysis for Planetary Gears. Modeling and Multibody Simulation

Hans Dresig
Institut für Mechanik, TU Chemnitz, D-09107 Chemnitz, Germany
e-mail: Hans.Dresig@mb.tu-chemnitz.de

Uwe Schreiber
ITI Gesellschaft für ingenieurtechnische Informationsverarbeitung mbH, D-01067 Dresden, Germany
Schreiber@iti.de

Abstract: For the development of robust, reliable, and smoothly running planetary gear stages the assessment of their vibration behavior and dynamical properties plays an important role already in the early design phases. This paper introduces a special sub-structure, which forms the base model for implementing all planetary gear configurations. Such models permit the dynamical simulation of planetary gearboxes with an arbitrary number of elastically mounted planets – considering the stiffness characteristics in the tooth contacts (including backlash and changing flank contacts) as well as all relevant toothing parameters (number of teeth, pressure angle, total engagement, addendum modification, etc.). By combining the base models with vibration models of the adjacent components in the drive a system simulation becomes possible, as well as the assessment of interactions with hydraulic or electro-mechanical components.

Keywords: Vibration; Planetary gear; Dynamical simulation; Modeling; Multibody system.

1   Introduction

The existing structures for planetary gearboxes have been systematically studied in the past and are well described in the literature (e.g. [3] and [7]). However, in this literature the structures are assembled from rigid bodies and only kinematic (and, with respect to inertia forces, kinetostatic) laws are taken into account. The modeling and simulation of elastic and vibratory planetary gearboxes up to now is often realized by using existing FEM or MBS tools ([5], [9]) or especially tailored programs such as SIMPLEX ([8], [10]), which maps planetary gearboxes with up to three stages as special cases of a „virtual gearbox".

Some of the existing programs can import stiffness data (bearings, shafts) from FEM programs, tooth contact stiffness characteristics from LVR [14] or KISSsoft [16], and geometries and mass parameters from CAD tools. As discussed in [4] and [9], the result visualization is also state of the art in the current construction development process.

Modeling methods and vibration analysis results are treated in [2] and [15]. From the extensive literature on the current research on vibrations in planetary gearboxes exemplarily [4] to [13] are mentioned, which all date to the last decade. So far, there does not exist a systematic approach for the modeling of elastic vibratory planetary gearboxes.

It is known by now, that the „elastic points" in planetary gearboxes are the coupling points between the gears (toothing and bearings). The varying tooth contact stiffness is a reason for the parametric excitations of vibrations, which in turn are significant causes for gearbox noises. Dynamic overloads, which are covered in general in DIN 3990, are also to be ascribed substantially to vibrations. In many cases the planetary gearboxes excite vibrations on the complete drive system, so that the coupling of the gearbox to neighboring components is of particular importance.

The authors of [5] and [8] point out, that the consideration of the tooth contact stiffness in the different contact points also requires the observation of the relative phase angles. They also give an estimation for noise excitations, which are influenced for instance by the torsional stiffnesses between the planet stages. In order to include the effects of tilting of particular gearbox components onto the load distribution along the tooth width, 3D computation models are required [10]. Such models require higher efforts in data provision, but in turn provide a more precise picture of the real load situations.

As the models mentioned in [9] and [10], the model in [11] contains the bearing stiffnesses fixed in the 3 coordinate directions in addition to the tangential tooth stiffnesses. The quantitative influence of the stiffness on the 18 natural frequencies and modes is shown in an example. [12] discusses the parametric excitations without considering elastic bearings and illustrates the influence of some toothing parameters onto the width of all instability regions.

One aim of this paper is to include the multitude of planetary gearbox structures into vibration simulation with a minimum modeling effort. The base model presented in the sequel covers the structures of all planetary gearboxes, with arbitrary combinations of internal and external toothings. This includes, e.g., the Wolfram gear set as well as the more complex Ravigneaux gear set [3]. The simulation models, which are assembled from the base model, can be evaluated and also combined with other model objects using the simulation software ITI-SIM [13], [17]. For the forced and parametrically excited vibrations the bearing stiffnesses are considered, but also the behaviorally important varying tooth contact stiffnesses, the phase angles of all toothings, the backlashes, and the flank contact changes during the oscillations. All interactions between tangential, radial, and axial directions are considered. All forces can be evaluated and displayed over time or via their spectra, as well as other

dynamic characteristics. This can be extended towards the computation of the load factors. The detailed vibration model is suitable for the analysis of the parameter influences relevant for the vibrations, which are of interest for the precise dimensioning of the planetary gearbox. All ITI-SIM interfaces, such as to FEM, MBS, and MATLAB/Simulink, can be used in the models.

2 Modeling of Arbitrary Planetary Gearbox Structures

2.1 Derivation of Common Base Structures for all Planetary Gearboxe

Due to the multitude of planetary gearbox structures the development of special model objects for each planetary gearbox type appears to be inefficient. Consequently, common base structures are searched for, from which all planetary gearboxes can be constructed.

According to the possible assembly of the central and planetary gears as external or internal toothing result eight different fundamental forms for planetary gears (Figure 1; e.g., [3] or [7]).
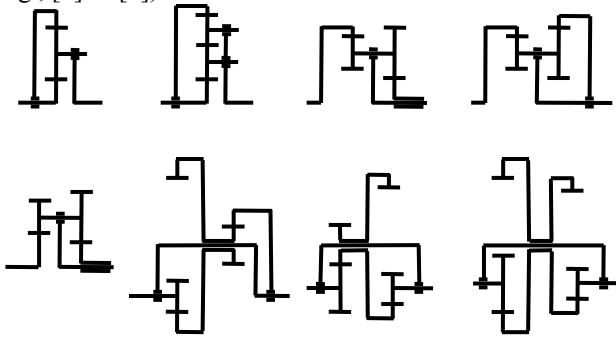

Figure 1 8 Fundamental Planetary Gearboxes

The smallest common substructure of planetary gearboxes (called „base structure" in the sequel) is composed of a central gear, a planet and the planet carrier. Depending on the toothing there exist 3 variants [13], which are depicted in Figure 2.
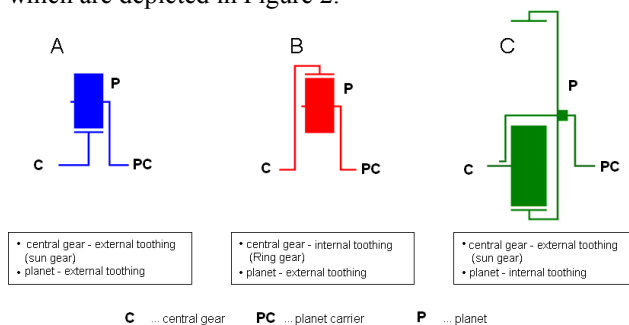

Figure 2   Variants for the base structure of planetary gearboxes

2.2 Model Object Implementation

The model objects to be developed shall become part of the system simulation software ITI-SIM [17]. This allows to model different properties of the system, such as the behavior of bearings or external components, outside of the base structure (cf. section 2.6). So the model objects to be implemented only have to compute the forces due to the elastic deformations at the teeth and to forward these to so called nodes. These nodes consider the inertia

properties of the respective parts (cf., e.g., Figure 5). The nodes compute from all acting forces F_e and the mass m the acceleration a (1) and, via integration, the velocities and displacements of the components:

$$a = \frac{\sum F_e}{m} \tag{1}$$

It is sufficient, to derive the mathematical background for one base structure only. The equations for the others differ in signs only. Using tooth numbers and axle distances with signs will result automatically in the correct formulations using just one set of equations (see e.g. [6]).

The tooth contact stiffness acts in the normal direction (coordinate direction x_{bn}). If the deformation at the tooth is multiplied by the contact stiffness, the result is the normal force in the contact. Here the current flank in contact (left or right) is estimated and delivers a force. Within the backlash there is no contact and the normal force is zero. If both flanks are in contact, both deliver a force. In the model it is checked first, which flanks are in contact and then the normal force F_{bn} is computed for each flank in contact according to (2), taking the backlash j_n and the stiffness k_{bn} into account. The resulting normal forces are then superposed. This algorithm covers all possible cases.

$$F_{bn} = \left(\Delta x_{bn} - \frac{j_n}{2} \right) \cdot k_{bn} \tag{2}$$

Apart from being able to use constant mean contact stiffnesses, the developed model objects also allow to consider stiffness variations during meshing. Several parameterization options, which are available on just a mouse click, are presented in the sequel.

All possible parameterizations use a function for the varying stiffness in the contact. For each tooth pair in contact the contact stiffness is determined in agreement with its phase angle. The total contact stiffness k_γ results from the superposition of the individual stiffnesses.

In order to compute the number of engaged teeth and the meshing position the angular difference $\Delta\varphi$ between the central gear and the planet must be known. In order to obtain the correct phase angle, the angle ς of the planet in the assembly has to be taken into account too

$$\Delta\varphi = \varphi_C - \varphi_O + \varsigma \tag{3}$$

The contact forces are computed separately for the left and the right tooth flank. A flank in contact delivers a non-zero force, so flank changes are easily observable. With respect to the stiffness, a one-sided contact results in the plain contact stiffness, whereas a double-sided contact also doubles the stiffness. If the is no contact, the teeth are in the backlash and the effective stiffness is zero.

2.3 Gearbox Modeling by Combining Base Structures

For all variants of the base structure, which are displayed in Figure 1, model objects were implemented. Figure 3 exemplarily shows the type A with all its connectors and their assignments.

The model objects themselves compute the forces and torques resulting from the deformations of the teeth and the elastic bearing of the planet on the planet carrier. All inertias are modeled externally using the adequate node objects. At the same time these nodes are the branching

points in the model structure, to which further elements or base structures can be connected. The combination of several base structures and the corresponding masses and inertias for the individual gears permits the modeling of all kinds of planetary gearboxes and the examination of all degrees of freedom relevant for the multibody system dynamics of the gearbox. As an example Figure 4 shows the simulation model for a Ravigneaux gear set, whose gear layout is displayed in Figure 5.

| No.	Connectable to	No.	Connectable to
1	Inertia of the central gear	7	Bearing of the central gear in x direction
2	Inertia of the planet carrier	8	Bearing of the planet carrier in z direction
3	Inertia of the planet with respect to its axis	9	Bearing of the planet carrier in y direction
4	Inertia of the planet with respect to its orbit	10	Bearing of the planet carrier in x direction
5	Bearing of the central gear in z direction	11	Node for the radial movement of the planet
6	Bearing of the central gear in y direction	12	Node for the axial movement of the planet
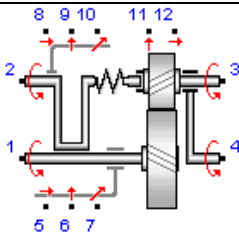
Figure 3   Symbol and connectors for the base structure type A model object
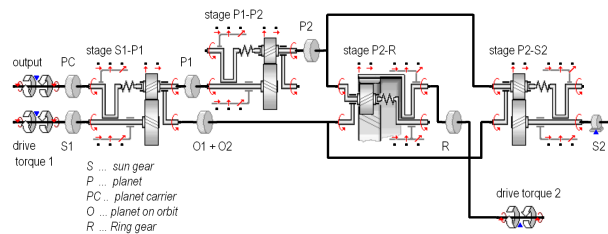

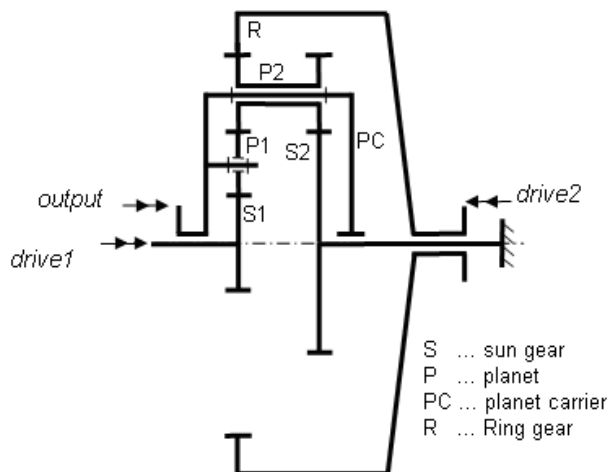**Figure 4   Simulation model for a Ravigneaux gear set, 2nd gear**

Figure 5   Structural layout of a planetary gearset according to Ravigneaux[3], 2nd gear

3   Example: Gearbox with 3 Planets
3.1   Computational Model

The model corresponds to the one presented in [12], where a varying stiffness in the tooth contact is considered, but the bearing stiffness is neglected. Figure 6 shows the respective gearbox layout and the corresponding ITI-SIM model structure.
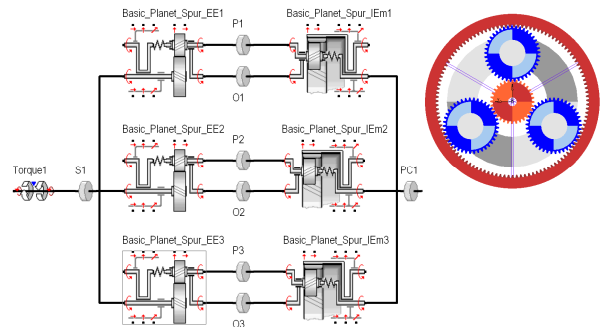

Figure 6   Gearbox layout and model structure for the discussed example

3.2   Main Instability Regions for Parametric Excitations

When providing a constant torque at the sun and simulating a run-up, the normal forces at the teeth are recorded as seen in Figure 7. The parametric excitation due to the varying stiffness in the tooth contact passes different resonance regions, where resonant responses and amplitude peaks are recorded.
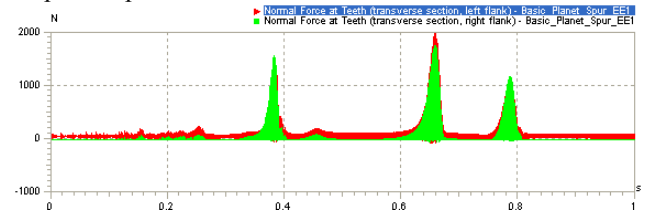

Figure 7 Normal tooth forces in a simulated run-up

A fast Fourier transformation (FFT) identifies the frequency components in these signals:
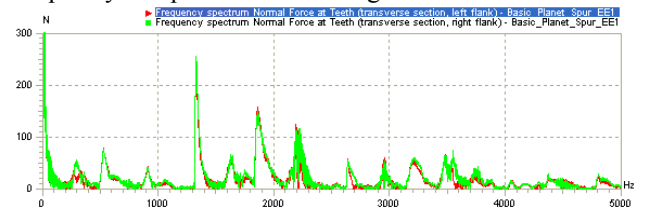

Figure 8 Spectra of the normal forces at the planet teeth

According to the theory ([12], [15]), the main instability region for parametric excitations is located around frequencies $f = 2\, f_i /n$ for small n (n = 1, 2, 3). Combined first-order resonances can occur at frequencies $(f_i + f_j)/n$ (in this case j = 2, 3, 4).

Figure 8 shows further oscillations with the following frequencies corresponding to the theory:

300 Hz $\approx f_2/4$; $f_3/6$; 620 Hz $\approx f_2/2$;

900 Hz $\approx f_3/2$; 1280 Hz $\approx f_2$;

1650 Hz $\approx (f_2 + f_3)/2$

1800 Hz $\approx f_3 \approx f_4$; 2200 Hz $\approx f_5$;

$2500\ \text{Hz} \approx 2\ f_2; 3250\ \text{Hz} \approx f_2 + f_3 \approx f_2 + f_4$

$3450\ \text{Hz} \approx f_2 + f_5; 3600\ \text{Hz} \approx 2\ f_3 \approx 2\ f_4.$

3.3 Influence of Tooth Contact Phase Angles on the Parametric Excitation Intensity

In the sequel the influence of the phase angles of the three tooth contacts is examined.

In the first case the planets are aligned symmetrically (all 120° apart from each other). The sun gear has 33 teeth, the ring gear 114. Thus, the three planets are engaged with one tooth in the sun gear as well as in the ring gear. The planets are located such, that the sum stiffnesses of all tooth contacts are in phase with respect to the sun gear. I.e., all minima and maxima of the stiffness curves coincide (Figure 9). The stiffness at the sun gear oscillates between $k = 0.8 \cdot 10^8$ and $1.3 \cdot 10^8$ N/m, which causes a strong parametric excitation due to the summation of the oscillation amplitudes of all stiffnesses.
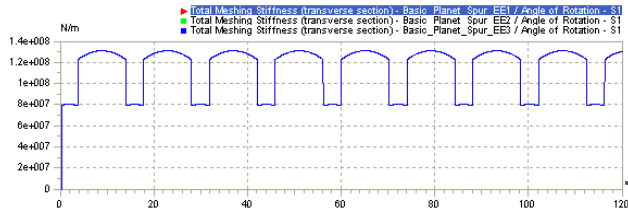
Figure 9 Synchronous change of all meshing spring stiffnesses for z_S=33, z_R=114, and 3×120°

In the second case the influence of the relative positions of the tooth contact points is studied. For this the planet axes are asymmetrically positioned. An offset is possible in the general, if the offset angle at the planet carrier integral multiple of the minimum angle δ_{min} ([3], [7]) amounts to.

$$\delta_{min} = 360\ °/(z_S + z_H) \qquad (4)$$

In the case of $z_S = 33$ teeth at the sun gear and $z_H = 114$ teeth at the ring gear results a minimum offset angle of

$$\delta_{min} = 360\ °/(z_S + z_H) = 2.4489\ °$$

So, if the planet carrier is not designed with three identical 120° angles, but with

$$\gamma_1 = 122.45\ °, \gamma_2 = 122.45\ °, \gamma_3 = 115.10\ °,$$

the vibration excitation in tangential direction will be reduced, whereas in radial direction there is no equalization anymore due to the disturbed symmetry. The resulting curve for the summated meshing stiffnesses is shown in Figure 10.
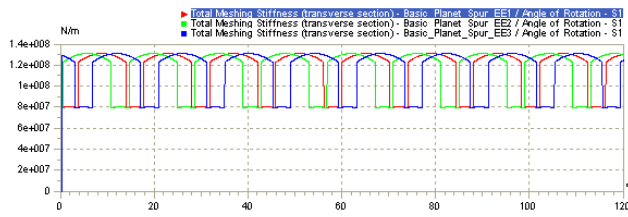
Figure 10 Meshing spring stiffnesses for z_S=33, z_R=114, and an agular offset according to (4)

For the two cases run-ups were simulated. In order to clearly assign resonances to the excitation orders, the simulation results were processed by an order analysis. The results are shown in Figure 11.
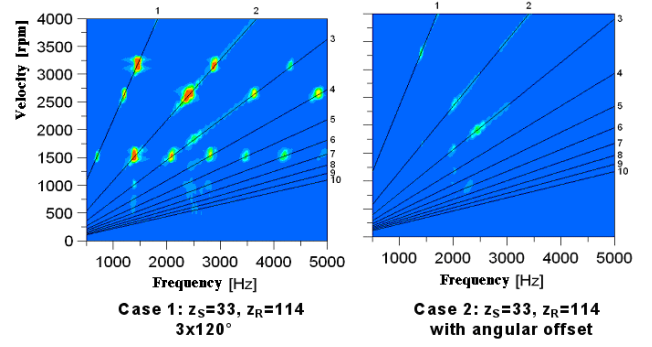
Figure 11 Order analysis results for the normal tooth contact forces in cases 1 and case 2

The inclined black lines in Figure 11 mark the orders (multiples) of the tooth meshing frequency f_{Eng}. This frequency can computed according to (5). It has to be taken into account that the number of teeth z_R of the ring gear has to bear a negative sign due to the internal toothing. n_S is the rotary speed of the sun gear in rpm and z_S the number of teeth on the sun gear

$$f_{Eng} = \frac{n_S}{60} \cdot \left(\frac{-z_R}{1 - \dfrac{z_R}{z_S}} \right) \qquad (5)$$

The excitation orders found in the signal over time appear as colored stripes along the order lines in the sonogram. The natural frequencies, which are present in the signal, are marked by amplitude rises, which are located on vertical lines in the diagram. Resonances can appear at all crossings between excitation order lines and natural frequency lines. The appearance of a resonance results in a colored spot at the crossing point, which indicates an amplitude rise. On the ordinate of the diagram the rotary speeds, at which the resonances occur, can be read off. In case 1 (left diagram in Figure 11) for instance, at sung gear speeds of about 1500 rpm there are resonances in the orders 1 to 7 of the tooth meshing frequency. In the signal over time (Figure 7) this corresponds to the rise in vibration amplitudes at about 0.39 s. Since the speed rises from 0 to 4000 rpm within one second, 1500 rpm are reached at about this time.

It is obvious, that due to the periodic (but not harmonic) tooth meshing in all cases the orders 1 to 7 of the excitation cause resonances, if a higher harmonic of the tooth meshing frequency coincides with a natural frequency of the gearbox. The natural frequencies are located at 1240 Hz, 1800 Hz, and 2200 Hz. It has to be pointed out, that here one encounters not resonances of forced vibrations, but the wider instability ranges of parametrically excited oscillations.

In case 1 the resonances appear at the frequencies, which were already identified via the FFT analysis in Figure 8. The resonances at a sun gear speed of 1500 rpm (meshing frequency ≈ 640 Hz) in case 1 corresponds to multiples of f2/2 ≈ 620 Hz, at 2600 rpm these are multiples of f5/2 ≈1100 Hz, and at 3100 rpm multiples of (f2 + f3)/2 ≈1450 Hz respectively.

Also in case 2 there is less oscillation in the tangential stiffness with respect to the sun gear due to the improvement in the meshing conditions after changing the angles. In consequence there are fewer resonance areas with less intensity compared to case 1. The 3rd and 4th natural frequencies are again subject to stronger excitations, because the excitation did not change from with respect to the planets.

It has to be pointed out in general, that modifications usually lead to improvements in one speed range only. A global improvement is not achievable. Usually the changes cause the appearance of new resonance regions. This can be observed in case 3, where such resonances arise between 4000 and 5000 rpm, which were not observable in case 1.

Further investigations showed, that the consideration of bearing stiffnesses reduces the natural frequencies and changes the corresponding mode shapes. The instability regions, which are already present for rigid bearings, become wider. Also, there appear new instability regions, which result in unbalanced bearing forces due to the translatory movement of the planets.

Further factors influencing the width and height of instability regions are the damping as well as the shape of the stiffness variation curve in the tooth contact.

4 Summary and Perspectives

An efficient method for modeling arbitrary planetary gearbox configurations, considering nonlinear tooth contact stiffnesses and the influence of the bearings in all coordinate directions in space, was presented. Based on typical examples the achieved simulation results were evaluated and discussed. The influence of different model parameters on the parametrically excited vibrations was analyzed. The three cases under study showed the particular influence of the relative phase in the gear meshing points on the intensity of the parametric excitations.

The results show, that the presented modeling approach is a practical and flexible method, which also leads to new insights into the behavior of the modeled systems. The developed models are suited for dimensioning tasks and the clarification of vibration causes (fault detection, diagnostics). In the near future the models are going to be used for the assessment of smoothness and operational reliability of planetary gearboxes, e.g., in gearboxes for passenger cars or wind turbines.

.

References

[1] Diekhans, G.: Numerische Simulation von parametererregten Getriebeschwingungen. RWTH Aachen: Dissertation 1981

[2] Kücükay, F.: Dynamik der Zahnradgetriebe. Berlin, Heidelberg, New York: Springer-Verlag, 1987

[3] Looman, J.: Konstruktionsbücher Band 26 – Zahnradgetriebe. Berlin, Heidelberg, New York: Springer-Verlag, 1988

[4] Dussac, M; Play,D.; Bard, D.R.: Design of Advanced Mechanical Systems, realistic Gear Dynamic Modelisation. VDI-Berichte 1230, S.115 -128. Düsseldorf: VDI - Verlag, 1996

[5] Gradu, M; Langenbeck, K.; Breunig, R.: Planetary Gears with Improved Vibrational Behaviour in Automatic Transmissions. VDI-Berichte 1230, S.861- 879. Düsseldorf: VDI-Verlag, 1996

[6] Linke, H.: Stirnradverzahnung. München/Wien: Hanser-Verlag, 1996

[7] Müller, H. W.: Die Umlaufrädergetriebe. Berlin, Heidelberg, New York: Springer-Verlag, 1998

[8] Quian, K.; W. Predki, W.; Jarchow, F.: Umlaufgetriebe mit Stufenplaneten. VDI Berichte 1460, S.317-334, Düsseldorf: VDI-Verlag, 1999

[9] Christ, M; Predki, W.; Jarchow, F.: Rechnersoftware für die integrierte Gestaltung und Berechnung von Planetengetrieben. VDI – Berichte 1460, S. 37 – 54, Düsseldorf: VDI-Verlag, 1999

[10] Polifke, G., Predki, W., Jarchow, F.: Simulation des dynamischen Schwingungs¬verhaltens mehrstufiger Planetengetriebe. VDI – Berichte 1460, S.297 – 316, Düsseldorf: VDI-Verlag, 1999

[11] Jian Lin; Parker, R.G.: Natural Frequency Veering in Planetary Gears. Mech. Struct. & Mach., 29(4), p. 411-429 (2001)

[12] Jian Lin; Parker, R.G.: Planetary Gear Parametric Instability Caused by Mesh Stiffness Variation. Journal of Sound and Vibration (2002) 249(1), p.129 – 145

[13] Butter, J.; Schreiber, U.: Modellierung von Planetengetriebestrukturen. 7. ITI Simulation Workshop, Dresden: 2004

[14] Börner, J.: LVR, Beanspruchungsverteilung an evolventischen Verzahnungen. Programm, TU Dresden: 2004

[15] Dresig, H.: Schwingungen mechanischer Antriebssysteme. Modellbildung, Berech¬nung, Analyse, Synthese. Berlin, Heidelberg, New York: Springer-Verlag, 2. Aufl., 2005

[16] www.kisssoft.ch

[17] Autorenkollektiv: ITI-SIM Handbuch. Dresden: ITI GmbH, 2005